Viscosity of periodic suspensions

Philippe Gondret, L. Petit

Viscosity of periodic suspensions

P. Gondret
Laboratoire Fluides, Automatique et Systèmes Thermiques (URA CNRS No. 871) Bât. 502, Campus Universitaire, F-91405 Orsay cedex, France

L. Petit
Laboratoire de Physique de la Matière Condensée (URA CNRS No. 190) Université de Nice, Parc Valrose, F-06108 Nice cedex 02, France

(Received 19 October 1995; accepted 29 May 1996)

By submitting macroscopic (non-Brownian) monodisperse suspensions of solid spheres to an oscillating shear flow with a ''rheo-optical'' set-up, a quasi-periodic ordering of spheres has been observed during the shearing motion, and viscosity measurements have been performed simultaneously. The viscosity values corresponding to the ordered suspensions are significantly smaller than the values corresponding to the disordered suspensions; they are compared with viscosity calculations made by other authors in the case of periodic suspensions of particles. © *1996 American Institute of Physics.* [S1070-6631(96)02509-3]

I. INTRODUCTION

The expression of the viscosity η of a suspension of solid spheres as a function of powers of the volume fraction ϕ of spheres was obtained up to the ϕ^2 term from the works of Batchelor and Green[1] extending those of Einstein[2] limited to the ϕ term. The main difficulty of treatment of non-dilute suspensions of particles comes from the existence of many-body hydrodynamic interactions between the particles. Even for the calculation of the ϕ^2 term corresponding to the pair-interactions,[1] the viscosity depends on the spatial distribution of the particles — the microstructure — which depends itself on the initial spatial distribution and on the nature of the flow (extensional flow, shear flow,...). No analytical calculation for the viscosity is available beyond this ϕ^2 term, because the distribution functions of more than two particles are not known.

To treat the case of concentrated suspensions another way is to consider a suspension with particles in a given spatial distribution, like periodic arrays of particles, and to calculate the macroscopic properties of the medium. Several authors developed expressions for the drag force in the case of different periodic arrays.[3–5] The methods employed for these calculations are quite often similar to the ones used for the calculation of the effective thermal conductivity in the case of periodic arrays of metallic spheres, or for the calculation of the effective elastic moduli of composite materials (periodic arrangements of spherical particles embedded in an isotropic matrix with different elastic properties).[4] Hasimoto[3] was probably the first to succeed in the treatment of the three kinds of cubic arrays [simple (SC), body-centered (BCC) and face-centered (FCC)] in the limit of low volume fractions, the extension to the whole range of volume fractions being made by Sangani and Acrivos.[4]

Later, new theoretical studies were made for the calculation of the viscosity of such periodic arrays of solid particles.[6–13] With the exact knowledge of the positions of all the particles it is possible to calculate the viscosity at all volume fractions by taking into account distribution functions of order as high as desired. The viscosity calculation of such periodic arrays may however appear rather academic. The reason is that the periodic arrays will be distorted by the flow. Therefore, the value of the viscosity will be valid only when the packing is cubical. The instantaneous value of the viscosity will be a periodic function of time. The effective value of the viscosity can be obtained by averaging the viscosity over all successive configurations of the lattice.

From an experimental point of view, many works report various structures induced by shear flow in colloidal suspensions (see, e.g., Ackerson[14] or Tomita *et al.*[15]), but few ones report similar results in the case of macroscopic, i.e., non-Brownian suspensions.[16,17] We performed viscosity measurements and visualizations of macroscopic suspensions of spheres with a rheo-optical set-up, and we measured the viscosity in two different states: an isotropic disordered state at the start of the flow and an ordered state, induced by the flow, characterized by a quasi-periodic spatial distribution of the particles.

The viscosity measurements of the disordered suspensions can be analyzed through effective medium models[18,19] following an idea first developed by Krieger and Dougherty.[20] Such an analysis has been done by several authors in the past and will therefore not be discussed in the present paper. More interesting is the case of the shear-induced quasi-periodically ordered suspensions observed in our experiments.[18,21]

The present paper gives the comparison between our experimental measurements and numerical calculations made by other authors[9,10,13] in the case of periodic suspensions of solid particles.

II. EXPERIMENTAL SET-UP

A. Fluid and particles

The suspensions we used are made of solid spheres embedded in a viscous fluid. The monodisperse glass beads (Potters Ballotini) of density $\rho_s = 2.5$ g cm^{-3} are obtained by mechanical sieving: the final diameters are in the range 45 ± 5 microns. The fluid used is a viscous silicon oil (Rhodorsil 47V5000, Rhône-Poulenc) known to have a small

 1070-6631/96/8(9)/2284/7/$10.00

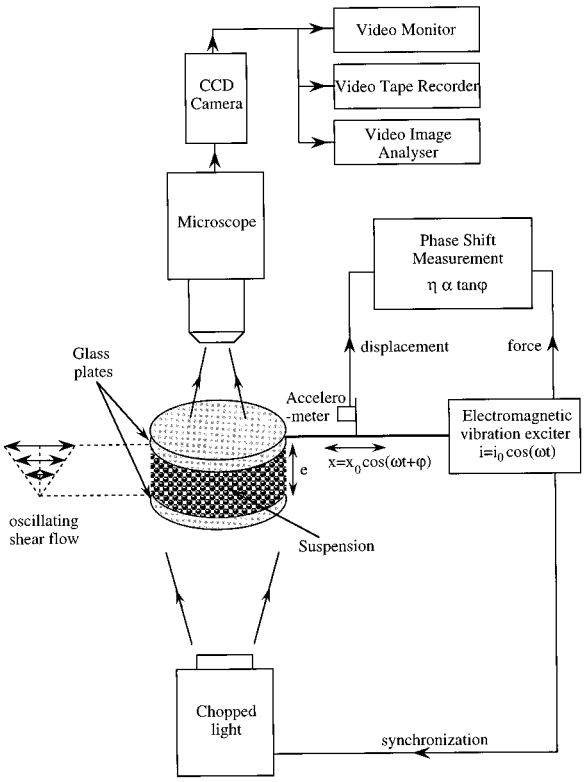

FIG. 1. Experimental set-up.

temperature dependence of the viscosity. Its viscosity is $\eta_f = 5$ Pa s at $T = 25\,^{\circ}\mathrm{C}$ and its density is $\rho_f = 0.97$ g cm^{-3}. The suspensions are homogenized by manually stirring the particles in the fluid and carefully avoiding bubble formation.

B. Type of flow

The suspension is confined between two parallel solid plates separated by a small gap ($e = 200$ μm) (Fig. 1). The lower plate is fixed and the upper one oscillates in one direction creating a simple shear flow in the fluid (frequency $f = \omega/2\pi = 200$ Hz; amplitude of displacement of the upper plate $x_0 \approx 20$ μm; shear rate $\dot{\gamma} = x_0\omega/e \approx 10^2$ s^{-1}). The shear rate is constant in the whole volume because the viscous penetration depth ($\delta = \sqrt{(2\eta_f)/(\rho_f\omega)} \approx 3$ mm) is much larger than the gap of the cell ($e \approx 200$ μm). The rate of strain γ does not vary either across the sample and is quite weak ($\gamma = x_0/e \approx 0.1$).

Considering the large sizes of the particles, the high viscosity of the suspending fluid and the amplitude of the shear flow, the particle Reynolds number is low ($\mathrm{Re} \approx 10^{-4}$) and the Péclet number is very high ($\mathrm{Pe} \approx 10^{11}$): Brownian forces as well as van der Waals and electrostatic forces between the particles can be neglected. Consequently, the particle interactions can be considered only as of hydrodynamic origin.

C. Optical set-up

The solid plates of the shear cell are made of transparent glass and the particles are observed by optical microscopy (Fig. 1). A chopped light synchronized at the excitation frequency allows us to observe only the slow movements of migration superimposed onto the applied oscillating flow. The microscope is connected to a video system composed of a CCD camera, a video monitor and a video tape-recorder; an image analysis is made on a computer.

D. Viscosity measurement

The viscosity is obtained from the phase shift between the alternative force applied to the upper plate to create the flow and the induced oscillating displacement of this plate (Fig. 1).

One signal is the electrical current in the electromagnetic vibrator: This signal is proportional to the force applied to the oscillating upper plate. The other signal is the output of an accelerometer fixed on the upper oscillating plate: This signal is proportional to the displacement of this plate. The phase shift φ between these two signals is measured by a lock-in amplifier, and stored in a computer as a function of the duration of the shear. This phase shift is directly related to the dynamic viscosity η of the fluid in the cell as it is demonstrated below.

If we note $i(t) = I_0 \cos(\omega t)$ the alternative current within the vibration exciter and $x(t) = A_0 \cos(\omega t + \varphi)$ the induced displacement of the upper plate, where $\omega = 2\pi f$ is the pulsation and f the frequency, the movement equation is

$$m\ddot{x} + \lambda\dot{x} + kx = Bli, \tag{1}$$

where m is the mass of the oscillating part, λ a viscous friction coefficient and k the restoring constant of the exciter. The right hand term Bli is the force that is proportional to the electric current i through the magnetic field B and the length l of the inducing wire. Written in complex form the equation is

$$-m\omega^2 A_0 + j\lambda\omega A_0 + kA_0 = BlI_0. \tag{2}$$

Then, the phase shift φ between the displacement x and the force Bli is

$$\tan\varphi = \frac{\lambda\omega}{k - m\omega^2} = \frac{-\lambda\omega}{m(\omega^2 - \omega_0^2)}, \tag{3}$$

where $\omega_0 = \sqrt{k/m}$ is the resonant pulsation of the system. The viscous friction coefficient λ can be related to the apparent viscosity η of the sheared fluid: The shear stress σ produced by the suspension on the upper plate being $\sigma = \eta\dot{\gamma} = \eta\dot{x}/e$, the viscous friction coefficient is $\lambda = \eta S/e$, where S is the shearing surface and e the gap between the two solid plates. The relation between the phase shift and the viscosity is therefore

$$\tan\varphi = \frac{-S\omega\eta}{m(\omega^2 - \omega_0^2)e}. \tag{4}$$

In fact, the measured phase shift $\tan\varphi$ is the sum of two terms: The first term is due to the viscosity of the sheared fluid and an additional term ($\tan\varphi_0$) is due to the viscous friction which is internal to the vibration exciter

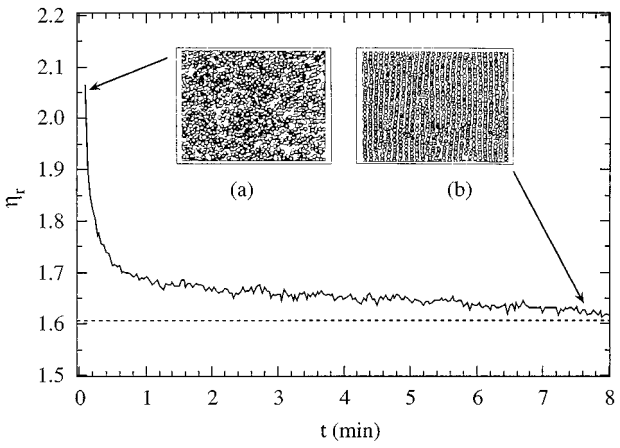

FIG. 2. Relative viscosity, η_r, of a monodisperse suspension of spheres (volume fraction $\phi=0.20$; particle diameter $d=45$ μm) as a function of the time t of shearing (frequency $f=200$ Hz; shear rate $\dot{\gamma}=100$ s^{-1}). The photo on the left side (a) shows the disordered suspension before shear, and on the right side (b) the ordered suspension after few minutes of shearing.

$$\tan\varphi=\frac{-S\omega\eta}{m(\omega^2-\omega_0^2)e}+\tan\varphi_0. \tag{5}$$

The measured apparent viscosity is therefore

$$\eta_{\text{app.}}=\frac{-m(\omega^2-\omega_0^2)e}{S\omega}(\tan\varphi-\tan\varphi_0). \tag{6}$$

The $\tan\varphi_0$ term is measured as a preliminary, with no fluid between the plates other than the air (for which the viscosity is neglected). In the case where the working frequency is much larger than the resonant frequency of the system ($\omega_0^2\ll\omega^2$), the relation giving the viscosity is simply

$$\eta_{\text{app.}}=\frac{m\omega e}{S}(\tan\varphi-\tan\varphi_0). \tag{7}$$

This is the case in our experiments since $f_0=48$ Hz and $f=200$ Hz. All this derivation is correct only if the sheared fluid is purely viscous. If the fluid has an elastic component, the elastic modulus can be determined by measuring the variation in the resonant frequency of the system. Such measurements have been done yet for electrorheological fluids with our experimental set-up.[22,23]

III. RESULTS AND DISCUSSION

A. Experimental results

The suspension placed between the plates is initially in a disordered state [see photo (a), Fig. 2]. As we applied the shear, we observe that the particles arrange themselves in periodic layers that are parallel to the plates and in periodic lines that are perpendicular to the plane of shear [see photo (b), Fig. 2]. The ordering time is of the order of few minutes, much greater than the characteristic time of the oscillating flow (period $T\approx10^{-4}$ s). The periodic ordering of the particles under an oscillating shear flow was first observed and interpreted by Petit and Noetinger.[24] The inertial secondary flows are induced by the alternating rotation of the particles under the oscillating shear flow. They result in attractive interactions between the particles along the axis of rotation and repulsive in the perpendicular equatorial plane. Despite the weakness of the inertial effects (Re$\ll$1), they are revealed because of their non-zero mean-value over long time by comparison with the period of the shear. The axis of rotation being perpendicular to the plane of shear, this explains the formation of lines of spheres at contact along this direction.

Indeed, the secondary flow around a rotating sphere due to small inertial effects in a viscous liquid can be found by using a perturbation method,[25] where the perturbation parameter that describes the importance of inertial effects is the Reynolds number $\text{Re}=\rho_f\Omega d^2/\eta$ that is based on the angular velocity Ω of the sphere. The inertial velocity v_i of this flow, which moves away from the sphere in the equatorial plane and towards the spheres along the axis of rotation, is therefore of the order of $v_i\sim\text{Re}\Omega d$. In a shear flow, a sphere rotates with an angular velocity $\Omega=\dot{\gamma}/2$ and the inertial velocity scales therefore as $v_i\sim\rho_f\dot{\gamma}^2d^3/\eta$. The time t_m for a particle to migrate over a distance of the order of its diameter is then:

$$t_m\sim\frac{d}{v_i}\sim\frac{\eta}{\rho_f\dot{\gamma}^2d^2}. \tag{8}$$

The $\dot{\gamma}^2$ dependence indicates that this velocity is the same whatever the direction of the flow: Any side the sphere could turn, the inertial flow is away from the sphere in the equatorial plane and to the sphere along the axis of rotation. The ρ_f dependence clearly indicates the inertial origin of this particle migration.

In our experiments $d\approx50$ μm and $\dot{\gamma}\approx100$ s^{-1} (Re$\approx5.10^{-5}$), so the time of inertial migration is $t_m\approx10^2$ s≈1 min. This value is effectively the typical time during which we observe by microscopy the migration of the particles forming at the end the parallel chains.

The migration we observe in this experiment is quite different from the diffusive process showed experimentally by Leighton and Acrivos[26] and modeled more recently by Philips *et al.*[27] and by Nott and Brady,[28] which occurs when the shear rate is non-homogeneous and at zero Reynolds number. In our experiments, the shear rate is homogeneous and the migration process is a function of the particle Reynolds number even if this number is low because of the cumulative effect due to the alternative movement.

Viscosity measurements performed simultaneously with microscopic visualization give the following results: As the shear is applied, we observe a significant decrease in the viscosity (Fig. 2). The viscosity starts from a given value and reaches an asymptotic lower value after a few minutes of shearing. This decrease is directly correlated with the ordering of particles described above, with a the typical time decrease of the order of 1 min. We observe this viscosity decrease and this particle ordering whatever the gap thickness (200 μm to 2 mm).

Thus, we define one viscosity $\eta_{r(t=0)}$ corresponding to the initial disordered state, and a second, lower viscosity, $\eta_{r(t=\infty)}$, corresponding to the final periodic ordered state. For all the solid volume fractions ϕ studied (up to 0.60), we

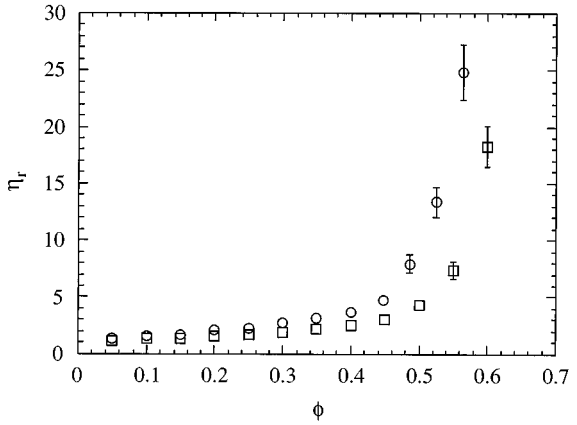

FIG. 3. Relative viscosity, η_r, of monodisperse suspensions of spheres (particle diameter $d=45$ μm) as a function of the volume fraction ϕ. (○): disordered suspensions before shear; (□): ordered suspension after 10 minutes of shearing.

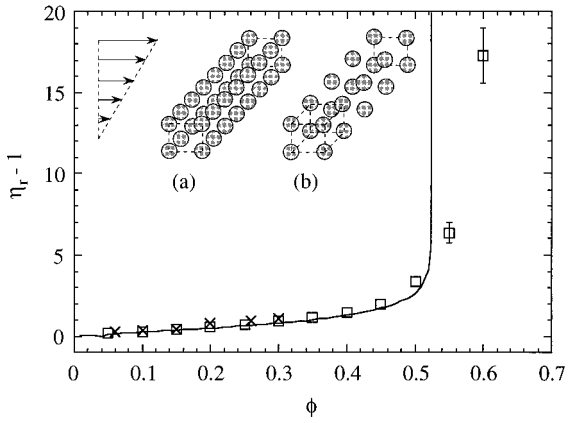

FIG. 4. Specific viscosity, η_r-1, of monodisperse suspensions of spheres (particle diameter $d=45$ μm) as a function of the volume fraction ϕ. (□): ordered suspension after 10 min of shearing; (—): numerical calculations for infinite S.C. suspensions of spheres made by Nunan and Keller (1984); (×): numerical calculations for S.C. suspensions of spheres made of just 3 layers parallel to the solid plates [Tran-Cong *et al.* (1990)]. Inside the graph are represented our shear-induced ordered suspensions (a) and the S.C. suspensions of spheres (b) relative to the simple shear flow (on the left).

observe this viscosity decrease: The viscosity of the disordered suspensions is always larger than the viscosity of the periodic ordered ones at the same volume fraction (Fig. 3).

In the following, we compare our viscosity measurements on ordered suspensions with numerical calculations made by other authors on periodic arrays of particles.

B. Periodic suspensions of spheres

The effective viscosity of a suspension of rigid spheres in an incompressible viscous fluid, with the spheres centered at the points of a periodic lattice, is defined to be the fourth-order tensor that relates the average deviatoric stress to the average rate of strain. In the case of the cubic symmetry, it reduced to the calculation of only two parameters. For the three cubic configurations (SC, BCC and FCC), these parameters have been numerically calculated by Nunan and Keller[9] at all volume fractions ϕ, from zero up to the close-packing value $\phi_{\max}$. Asymptotic formulae have also been obtained by Zuzovsky *et al.*[8] in the limit of low concentrations, and by Nunan and Keller[9] for high concentrations. In the case of the simple-cubic array, the asymptotic formulae are the following:

$$\eta_r(\phi)=1+\frac{5}{2}\,\frac{\phi}{1+0.862\phi-2.286\phi^{5/3}}\quad\text{when}\quad\phi\to 0, \tag{9}$$

$$\eta_r(\phi)=0.37-\frac{\pi}{4}\ln\left(1-\left(\frac{\phi}{0.524}\right)^{1/3}\right)\quad\text{when}\quad\phi\to\phi_{\max}. \tag{10}$$

One can verify that relation (2) gives the correct coefficient (5/2) for the linear term in the volume fraction for the very dilute regime. In the concentrated regime, relation (3) indicates that the viscosity goes to infinity when the volume fraction of the simple cubic suspensions approaches the maximum volume fraction ($\phi_{\max}$(S.C.)$=0.524$) of this array.

The quasi-periodic ordering of our sheared suspensions leads us to make comparison between the viscosity measurements and numerical calculations on periodic suspensions of spheres in simple cubic array (S.C.) (Fig. 4).

The comparison is rather good for volume fractions up to about 50%. For larger volume fractions, there is a sudden discrepancy between the two curves. The reason is that the viscosity of the S.C. suspensions diverges drastically as the packing fraction of this array is approached ($\phi_{\max}$(S.C.)$=0.524$), but the structure of our quasi-periodic suspensions is not exactly the simple cubic-array. The main difference between the structures we observed [insert (a), Fig. 4] and the pure SC structures [insert (b), Fig. 4] is that the particles in the former are in contact in the direction that is perpendicular to the plane of shear. Nevertheless, the rather good agreement up to 50%, may come from the fact that the spheres in this direction do not strongly interact because there is no relative motion between them: Consequently, the spacing between these spheres is unimportant in this direction.

Another question that can be raised is the relevance of dependence on the size of the system. In the numerical calculations of Nunan and Keller discussed above, the suspension is supposed to be infinite in size, without boundary effects. On the contrary, in our experiments, the suspension is of finite size since it is limited by two parallel solid plates. We will now examine the variation in the viscosity of a periodic suspension due to its confinement between two shearing parallel solid walls.

Tran-Cong *et al.*[10] performed numerical calculations in such cases: the suspensions they considered are made of only few layers of particles (typically one to four layers) that are parallel to the wall and regularly spaced. Their results show that, for a given volume fraction, the viscosity increases when the number of layers increases (the spacing between

the walls is enlarged to keep the volume fraction constant), but this enhancement saturates very rapidly as soon as few layers are stacked one over the other: For the largest volume fraction they studied ($\phi = 0.315$), the viscosity differs by only 5% between the two- and three-layered suspensions and reduces to 1.5% between the three- and four-layered suspensions. The conclusion is that a three- or four-layered suspension is sufficient to reproduce a periodic suspension in three directions.[10] In our experiment, the spacing between the two shearing plates is $e = 200$ μm. Considering the particle diameter ($d = 45$ μm), the number of layers is of the order of 3 or 4 depending on the volume fraction. The reason for which we made our experiments with this small spacing is that the visualization is easier. However, we observe the same ordering and viscosity decrease if the spacing is much higher. Although the calculations of Tran-Cong *et al.* are not available at volume fractions higher than 0.3, one can see (Fig. 4) that the agreement of our experimental results ($\square$) with the numerical ones ($\times$) is very satisfactory. The limited extension of the shearing cell is therefore not very important in the case of periodic suspensions, provided that exists more than 3 layers in the gap.

In our shear-induced ordered suspensions, the spheres are aligned in close contact in one particular direction and the particles of each line do not rotate independently but as a whole: another way is to compare these chains of spheres with elongated bodies. Such a comparison is exposed in the following section.

C. Periodic suspensions of prolate spheroids

Bibbo *et al.*[27] made some experiments with a parallel-plate rheometer on suspensions of non-Brownian fibers: There is a rapid viscosity decrease as the strain is increased, this decrease being correlated with a strong change in the orientational distribution, from an initial state with a random distribution to a final state in which most of the fibers are aligned in the shearing planes. For instance, the relative viscosity of fiber suspensions of aspect ratio $r_p \approx 17$ (length-to-thickness ratio) at volume fraction $\phi \approx 0.10$ decreases from roughly 4 to 1.5, i.e., decreases by 60%. In our previously described experiments, the relative viscosity of suspensions of spheres associated with the disordered-ordered ''transition'' decreases only by a 15% factor at the same volume fraction. In the case of fibers, the effect is reinforced by the anisotropy of the particles.

The comparison of a chain of spheres at close-contact with a prolate spheroid [see Figs. 5(a) and 5(b)] have been made recently by Zahn *et al.*[30] for a sedimentation problem at very low particle Reynolds numbers. Using magnetic field induced aggregation of paramagnetic colloidal spheres into linear chains of calibrated length, they determine the anisotropic friction coefficients of the chains, with a range from 1 to 100 particles, by video-microscopic observation of sedimentation velocity. The results they found agree well with the Slender-body theory (valid for thin elongated bodies of various shapes but of vanishing thickness-to-length ratio) even with small chains lengths. At low Reynolds number, the velocity field far from an object do not depend strongly on its shape. In the case of suspensions of solid particles, the effective viscosity depends also only slightly on the particle shape at volume fractions sufficiently lower than the maximum packing fraction.[11]

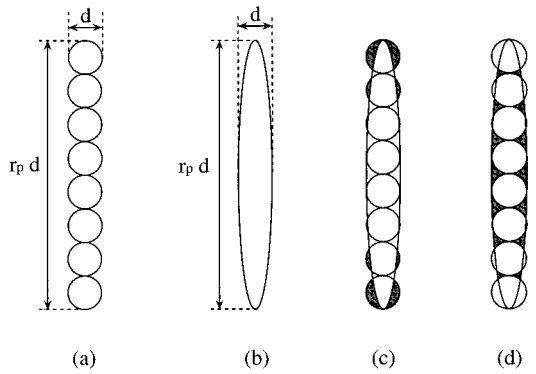

FIG. 5. Illustrations of (a) a line of $r_p = 8$ spheres of diameter d; (b) a prolate spheroid of aspect ratio $r_p = 8$ (length $r_p d$ and diameter d); (c) the shaded areas represent the loss of solid matter for a prolate spheroid relative to a chain of spheres of same aspect ratio; (d) the shaded areas represent the extra solid matter of a prolate spheroid relative to a chain of spheres of same aspect ratio. The sum of the shaded areas appearing respectively in (c) and (d) are equal, meaning that the volume of the two objects are equal.

A suspension made of n lines of p spheres of diameter d per unit volume has the same solid volume fraction as a suspension made of the same number n of prolate spheroids of the same aspect ratio $r_p = p$ (length $L = pd$, diameter d). The reason is that the volume $V_{\text{p.s.}}$ of a prolate spheroid of aspect ratio p ($V_{\text{p.s.}} = \pi(pd)d^2/6$) is surprisingly equal to the volume $V_{\text{c.p.}}$ of a chain of p spheres ($V_{\text{c.n.}} = p\pi d^3/6$). The extra solid matter of the spheroids filling the holes between the spheres at close contact [shaded area, Fig. 5(d)] balances exactly its loss of matter at each thin tip [shaded area, Fig. 5(c)]!

The behavior of suspensions of anisotropic bodies submitted to a given flow is even much more complex than the case of suspensions of spheres since in addition the distribution of particle orientations must be taken into account. In simple shear flows, an elongated particle does not have an equilibrium position, but experiences a periodic rotating motion, spending however much of its time aligned in the velocity direction. Hence, a suspension of elongated particles that is in an initially random distribution of orientation and that is submitted to this flow will do not remained random if Brownian motion can be neglected. To succeed in the viscosity calculation, one has to know on one hand the statistic distribution of the particle orientations, and on the other hand the stress contribution for each orientation. The problem appears therefore extremely complex. Roughly speaking, the increase of the viscosity due to the presence of elongated bodies (length L, width $d = L/r_p$) is proportional to nL^3 ($= \phi r_p^2$) with arbitrarily chosen orientation distribution, to $nL^2 d$ ($= \phi r_p$) if all particles are in the plane of shear and to nLd^2 ($= \phi$) if particles are perpendicular to the plane of shear. More exactly, theories exist in the dilute limit ($nL^3 \ll 1$ or $\phi \ll r_p^{-2}$) even for suspensions of particle of finite aspect ratio[31] but the theories developed in semi-dilute regime ($nL^2 d \ll 1$ or $\phi \ll r_p^{-1}$) are in the Slender-body approxi-

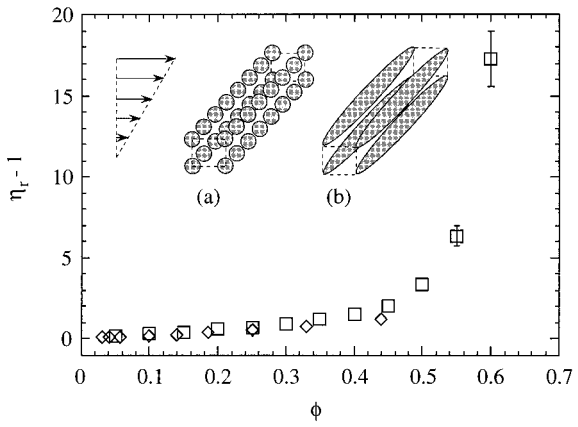

FIG. 6. Specific viscosity, $\eta_r - 1$, of monodisperse suspensions of spheres (particle diameter $d = 45$ μm) as a function of the volume fraction ϕ. (□): ordered suspension after 10 min of shearing; (◇): numerical calculations for S.C. array of suspensions of prolate spheroids by Claeys and Brady (1993). Inside the graph are represented our shear-induced ordered suspensions of spheres (a) and the S.C. suspensions of prolate spheroids (b) relative to the simple shear flow (on the left).

mation, i.e., in the case of an infinite aspect ratio.[32] In the case where all the fibers are perpendicular to the plane of shear, these theories do not give a viscosity increase as a function of the fiber volume fraction since the thickness of the fibers is supposed to be zero.

Another approach is the numerical calculations made by Claeys and Brady[13] for the effective properties of suspensions of rigid non-Brownian prolate spheroids interacting hydrodynamically in a Newtonian, incompressible fluid at zero Reynolds number, by taking into account not only the far-field interactions but also the lubrication effects. In particular they calculate the viscosity of crystalline dispersions of these elongated particles. The relative viscosity is given by the relation[13]

$$\eta_r = 1 + 6kr_p^2\phi, \tag{11}$$

where k is a numerical coefficient that depends on the spatial distribution of the spheroids, on the aspect ratio, on the type of the flow (pure strain, pure shear,...) and on the solid volume fraction ϕ. The parameter r_p^2 is used to emphasized the anisotropy of the spheroids: the volume fraction $\phi^* = r_p^2\phi$ would be the effective volume fraction of a suspension where spheres of diameter $d^* = r_p d$ would replace the prolate spheroids of aspect ratio r_p. These authors calculate the numerical value of the coefficient k as a function of the volume fraction, for several kinds of regular arrays containing spheroids of aspect ratio $r_p = 8$ and submitted to different types of flows. We have taken their values of k corresponding to prolate spheroids arranged in the expanded simple cubic array (e.s.c.) and submitted to a simple shear flow in a plane perpendicular to the spheroids, with the undisturbed velocity lying along the shortest vector of the lattice [see schematic illustration (b) in the insert of Figure 4]. This corresponds very well to our experimental suspension microstructure and to our flow conditions [insert (a), Fig. 6]. The e.s.c. structure is obtained from a simple cubic close-packing of spheres by stretching it along the main crystallographic direction (100) by a factor equal to the aspect ratio of the spheroids: This transformation maps a sphere onto a spheroid without altering the volume fraction [Figs. 5(c) and 5(d)]; then, different volume fractions can be obtained by an isotropic dilution of this dense microstructure while keeping the surface-to-surface separation between nearest neighbors the same in the three main perpendicular directions. Such a technique is adopted to achieve the same packing fraction as the one of the simple cubic cell of spheres ($\phi_{\text{e.s.c.}} = \phi_{\text{s.c.}} = \pi/6 = 0.52$). Otherwise, a simple cubic array of prolate spheroids of aspect ratio r_p is in such a way that the center-to-center separations are the same in the three perpendicular directions but not the surface-to-surface separations; its packing fraction is therefore equal to $0.52/r_p^2$. This would lead to a drastic decrease in the maximum packing fraction: For aspect ratio $r_p = 10$, the highest volume fraction attainable would be equal to 0.005.

Figure 6 shows that the numerical calculations of these periodic suspensions of prolate spheroids correspond quite well with our viscosity measurements of ordered suspensions of spheres. This agreement means that the differential rotation between touching particles in each chain is unimportant. Unfortunately, the calculations have not been done beyond a volume fraction of 45%. Such a concentration is however extremely high if we remember that volume fractions investigated experimentally for disordered suspensions of fibers do not exceed 30%. At $\phi = 0.45$, $nL^2d \approx 1$, which is the limit between semi-dilute and concentrated regime.

IV. CONCLUSION

The experiments we performed show the advantage lying in the use of a rheo-optical set-up in the case of complex fluids: we could correlate the macroscopic behavior of suspensions of solid spheres (by viscosity measurements) with the microstructure (by optical microscopy).

In addition, we found a good agreement between our viscosity measurements for the quasi-periodic shear-induced suspensions we observed and viscosity calculations of suspensions of particles ordered in perfect regular arrays. This comparison reinforced the interest of simulations of ordered systems.

ACKNOWLEDGMENTS

The experiments were performed in the Laboratoire de Physique de l'Ecole Normale Supérieure de Lyon (URA CNRS n°1325), in the frame of the G.d.R. C.N.R.S. ''Physique des Milieux Hétérogènes Complexes.'' The authors are grateful to Michel Cloître for fruitful discussions on fiber suspensions.

[1] G. K. Batchelor and J. T. Green, ''The determination of the bulk stress in a suspension of spherical particles to order c^2,'' J. Fluid Mech. **56**, 401 (1972).

[2] A. Einstein, ''Eine neue Bestimmung der Molekuldimension,'' Ann. Phys. **19**, 286-306 (1906); ''Berichtigung zu meiner Arbeit: Eine neue Bestimmung der Molekuldimension,'' *ibid.* **34**, 591 (1911).

[3] H. Hasimoto, ''On the periodic fundamental solutions of the Stokes equations and their application to viscous flow past a cubic array of spheres,'' J. Fluid Mech. **5**, 317 (1959).

[4]A. S. Sangani and A. Acrivos, ''Slow flow through a periodic array of spheres,'' Int. J. Multiphase Flow **8**, 343 (1982).
[5]A. A. Zick and G. M. Homsy, ''Stokes flow through periodic arrays of spheres,'' J. Fluid Mech. **115**, 13 (1982).
[6]N. A. Frankel and A. Acrivos, ''On the viscosity of a concentrated suspension of solid spheres,'' Chem. Eng. Sci. **22**, 847 (1967) .
[7]R. Kapral and D. Bedeaux, ''The effective shear viscosity of a regular array of suspended spheres,'' Physica A **91**, 590 (1978).
[8]M. Zuzovsky, P. M. Adler, and H. Brenner, ''Spatially periodic suspensions of convex particles in linear shear flows. III. Dilute arrays of spheres suspended in newtonian fluids,'' Phys. Fluids **26**, 1714 (1983).
[9]K. C. Nunan and J. B. Keller, ''Effective viscosity of a periodic suspension,'' J. Fluid Mech. **142**, 269 (1984).
[10]T. Tran-Cong, N. Phan-Thien, and A.L. Graham, ''Stokes problems of multiparticle systems: periodic arrays,'' Phys. Fluids A **2**, 666 (1990).
[11]N. Phan-Thien, T. Tran-Cong and A.L. Graham, ''Shear flow of a periodic array of particle clusters: a boundary-element method,'' J. Fluid Mech. **228**, 275 (1991).
[12]B. H. A. A. Van den Brule and R. J. J. Jongschaap, ''Modeling of concentrated suspensions,'' J. Stat. Phys. **62**, 1225 (1991).
[13]I. L. Claeys and J. F. Brady, ''Suspensions of prolate spheroids in Stokes flow. Part 3. Hydrodynamic transport properties of crystalline dispersions,'' J. Fluid Mech. **251**, 479 (1993).
[14]B. J. Ackerson, ''Shear induced order and shear processing of model hard spheres suspensions,'' J. Rheol. **34**, 553 (1990).
[15]M. Tomita and T. G. M. van de Ven, ''The structure of sheared ordered lattices,'' J. Colloid Interface Sci. **99**, 374 (1984).
[16]R. Pätzold, ''Die Abh'ángigkeit des Fliessverhaltens konzentrierter Kugelsuspensionen von der Strömungsform: Ein Vergleich der Viskosität in Sher- und Dehnströmungen,'' Rheol. Acta **19**, 322 (1980).
[17]D. J. Highgate and R. W. Whorlow, ''End effects and particle migration effects in concentric cylinder rheometry,'' Rheol. Acta **8**, 142 (1969).
[18]P. Gondret, ''Hydrodynamics of monodisperse and bidisperse suspensions under oscillating shear flow,'' Ph.D. Thesis, University of Lyon, 1994 (in French).
[19]P. Gondret and L. Petit, ''Viscosity of disordered and ordered suspensions of solid spheres: experimental results and models,'' C. R. Acad. Sci. Paris II **321**, 25 (1995).
[20]I. M. Krieger and T. J. Dougherty, ''A mechanism for non-newtonian flow in suspensions of rigid spheres,'' Trans. Soc. Rheol. **3**, 137 (1959).
[21]P. Gondret and L. Petit, ''Crystallization of macroscopic suspensions under shear: influence of particle size distribution,'' Europhys. Lett. **22**, 347 (1993).
[22]G. Bossis, E. Lemaire, J. Persello, and L. Petit, ''Structuration and elasticity of electrorheological fluids,'' Prog. Coll. Polym. Sci. **89**, 1 (1992).
[23]G. Bossis, Y. Grasselli, E. Lemaire, J. Persello, and L. Petit, ''Phase separation and flow-induced anisotropy in electrorheological fluids,'' Europhys. Lett. **25**, 335 (1994).
[24]L. Petit and B. Noetinger, ''Shear-induced structures in macroscopic dispersions,'' Rheol. Acta **27**, 437 (1988).
[25]R. B. Bird, R. C. Armstrong, and O. Hassager, *Dynamics of Polymeric Liquids. Volume I: Fluid Mechanics* (Wiley, New York, 1987), p. 31.
[26]D. Leighton and A. Acrivos, ''The shear-induced migration of particles in concentrated suspensions,'' J. Fluid Mech. **181**, 415 (1987).
[27]R. J. Philips, R. C. Armstrong, R. A. Brown, A. L. Graham, and J. R. Abbott, ''A constitutive equation for concentrated suspensions that accounts for shear-induced particle migration,'' Phys. Fluids A **4**, 30 (1992).
[28]P. Nott and J. F. Brady, ''Pressure-driven flow of suspensions: simulation and theory,'' J. Fluid Mech. **275**, 157 (1994).
[29]M. A. Bibbo, S. M. Dinh, and R. C. Armstrong, ''Shear flow properties of semiconcentrated fiber suspensions,'' J. Rheol. **29**, 905 (1985).
[30]K. Zahn, R. Lenke, and G. Maret, ''Friction coefficient of rod-like chains of spheres at very low Reynolds numbers. I. Experiment,'' J. Phys. II (Paris) **4**, 555 (1994).
[31]G. K. Batchelor, ''The stress generated in a non-dilute suspension of elongated particles by pure straining motion,'' J. Fluid Mech. **46**, 813 (1971).
[32]E. S. G. Shaqfeh and G. H. Fredrickson, ''The hydrodynamic stress in a suspension of rods,'' Phys. Fluids A **2**, 7 (1990).